cases. This finding may suggest that, at small angles of attack, lift and wake-collapse sources of internal wave generation might be usefully considered as uncoupled.

The early trajectory of the wake centerline is fairly well predicted by the self-similar theory of Tulin and Shwartz, using reasonable values for the empirical parameters involved. The maximum excursion occurs prior to the onset of collapse.

Acknowledgments

The work was supported by the U.S. Navy Space and Naval Warfare Systems Command under Contract N00039-89-C-5301. The formulation of the linear solution for the propagation of lift-generated internal waves used here was first carried out by J. J. Riley, D. R. S. Ko, and R. E. Robins at Flow Research Company, Kent, Washington. The efforts of C. L. Yates, C. R. Walton, A. Brandt, and G. Dailey in helping to conduct the experiments and analyze the experimental data are much appreciated.

References

[1]Gilreath, H. E., and Brandt, A., "Experiments on the Generation of Internal Waves in a Stratified Fluid," *AIAA Journal*, Vol. 21, No. 5, 1985, pp. 693–700.

[2]Thwaites, B., *Incompressible Aerodynamics*, Oxford Press, London, 1960.

[3]Tulin, M. B., and Shwartz, J., "The Motion of Turbulent Vortex Pairs in Homogeneous and Stratified Media," Hydronautics, Inc., Tech. Rept. 231-13, Laurel, MD, April 1971.

Surface Grid Generation Based on Unstructured Grids

Masahiro Suzuki*

Institute of Computational Fluid Dynamics, Tokyo, Japan

Introduction

IT has been well recognized that the generation of surface grids for complex configurations requires a great deal of human labor, although the computational expense of setting up surface grids may not be prohibitive. Naturally, effective generation of surface grids has been the subject of considerable attention in the literature. The general methods to produce the grids for three-dimensional flowfields are numerous; however, the present capabilities of generating the surface grids are limited in scope and versatility. At this time, the generation techniques for surface grids are of two general types: 1) numerical solution of partial differential equations (PDE) and 2) algebraic interpolation. In general, both systems treat generating the surface grid as a two-dimensional boundary-value problem on a curved surface, which is specified by a quadrangular patch through the use of surface parametric coordinates. The generation of the surface grid is accomplished over several stages. First, the Cartesian coordinate values $r_{i,j}$ of the boundary points on the four edges of the surface grid are specified, converting these values to the surface parametric coordinate values $(u_{i,j}, v_{i,j})$ on the edges. Then, the interior values in the array $u_{i,j}$ and $v_{i,j}$ from the edge values are determined by interpolation or PDE solution. Finally, these parametric coordinate values are converted to the Cartesian coordinates $r_{i,j}$. This procedure requires a well-structured surface for the input data. In view of this stringent requirement, conventional surface grid generation is inefficient and laborious. In practice, the preparation of a large amount of input data is an extremely time-consuming task. The geometry data for complex configurations, which are often utilized in engineering applications, are customarily produced by use of a computer-aided design (CAD) system. Under idealized conditions, accurate input data for the surface definition would be available directly from the CAD package. However, in reality, the currently existing CAD software programs are, by and large, incapable of providing this vital information. At the present level of development, a series of cross sections, i.e., the one-dimensional arrays of x, y, and z coordinates, are usually extracted from the CAD package. It is important to note that these data are primitive or raw. The points sets or distributions vary widely among cross sections. The conventional surface grid generator needs a quadrangular patch for the input data of the geometry definition as mentioned earlier; these primitive data must be grouped into quadrangular patches, which constitute the basis for a global patch. For this purpose, several data processors, which use some forms of interpolation, have been developed.[1,2] However, it is difficult to connect the local patches and to lap a quadrangular patch around the computationally complex geometry. This geometry does not necessarily represent a whole body, but it denotes a surface in which one coordinate is kept constant. If the local patches cannot be connected into a global patch, the grids are generated on each local patch, and then these grids can be combined. Therefore, to ensure continuity of the slope and curvature between each block, special treatments are essential.

It is easier and more flexible to describe a complicated geometry by plural polygonal surface patches (referred to as the unstructured grid) rather than by a quadrangular patch. Consequently, it would be highly advantageous if a way could be found in which the unstructured grid could be utilized directly for surface grid generation. From this point of view, investigations have been pursued to devise a scheme based on the unstructured grid. In the present study, the basic idea of constructing the surface grid is similar to the two-dimensional grid generation technique of Rao et al.[3] They proposed a methodology using Laplace's equations, which are solved in the physical domain using the finite element technique. The curvilinear coordinate lines are constructed by utilizing the interpolation functions applicable within each element, and the grid inside the solution domain is produced. Thus, in contrast to the well-known elliptic grid generation equations solved in the computational domain,[4] the method of Ref. 3 avoids the need to solve nonlinear equations, and the orthogonality is satisfied. The implementation of the Dirichlet or Neumann boundary conditions, which relate to the grid spacing and the slope of grid lines at the boundary, is straightforward. Reference 3 employed the quadrangular element, and no efforts were made to create the structured grid from the unstructured grid. Rao et al. point out only the advantage of solving the Laplace equations in the physical domain. In the present work, the unstructured grid is introduced to solve Laplace's equations. This unstructured grid specifies the three-dimensional surfaces. The curvilinear coordinate lines are drawn by searching for the contours inside the solution domain, i.e., the three-dimensional surfaces, to produce the surface grids. By introducing the weighting function, as asserted by Thompson et al.,[4] the grid space control is also achieved.

Model

Finite Element Solution Procedure

The following PDEs are mapped and solved by a finite element method on the unstructured grid:

$$\nabla(\lambda \nabla \xi) = 0 \qquad (1)$$

$$\nabla(\lambda \nabla \eta) = 0 \qquad (2)$$

Received July 5, 1990; revision received Nov. 6, 1990; accepted for publication Nov. 9, 1990.

*Research Staff, 1-16-5 Haramachi, Meguro-ku, 152. Member AIAA.

where λ is a weight function. The Galerkin's weighted residual approach is employed. The incomplete Cholesky decomposition conjugate gradient method[5] is used to solve the linear system of equations. In conjunction with solving the linear equations, this solver reduces substantially the CPU time in comparison with the common direct method. The solution contours of each equation define the curvilinear coordinate lines of ξ and η, respectively. Therefore, the boundary conditions specify the topology of the surface grid. In the two-dimensional grid generation, only the attraction of coordinate lines to boundaries is usually required, with the exception of the case of the adaptation to the flow solution. However, additional considerations are called for in three-dimensional flow calculations. The surface grid itself forms the boundary in the three-dimensional flowfield; therefore, it is imperative to achieve the attraction of coordinate lines to the interior fixed areas rather than on the edge boundaries. The attraction areas, e.g., big curved segments of the surface, are specified in the physical domain in the case of the initial grid generation, not in the case of the flow solution adaptation. Since the equations are solved in the physical domain, the control of the grid space can be implemented directly by using the weight function λ. As λ increases, the gradient of the solution decreases; i.e., the grid spacing becomes large. In practice, the weight function can be related to the curvature of the surface or the distance from the boundaries.

Surface Grid Construction

To obtain the surface grid, the curvilinear coordinate lines are constructed by searching for the contours inside the solution domain (Fig. 1). It does not take much computational time to search for the contours; the network information of the unstructured grid and a hierarchical data structure, i.e., three levels of data (points, lines, and patches), are executed in advance. The intersections of each coordinate line are acquired by the same order of interpolations as that of the patch within each element.

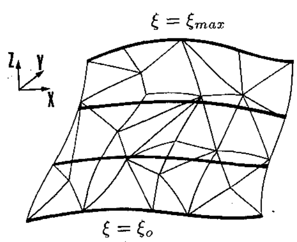

a) Construction of ξ-const lines

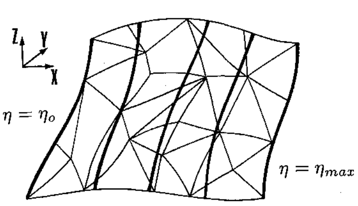

b) Construction of η-const lines

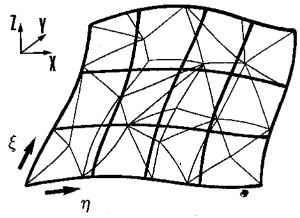

c) Surface grid

Fig. 1 Construction of surface grid. (Part c is obtained by combining parts a and b.)

Examples

In the method described herein, the unstructured grid can contain several types of patches, e.g., C^1-continuous/C^2-continuous triangular/quadrangular surface patches. For simplicity, however, the linear triangular surface patch was selected as an example. To demonstrate the capability of the present method, several illustrative configurations have been tested.

The advantage of dealing with plural surface patches is shown clearly in Fig. 2. The H-type grid is made on a pyramid. The geometry has discontinuities. It is considerably diffi-

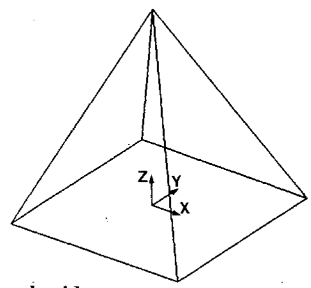

a) Unstructured grid

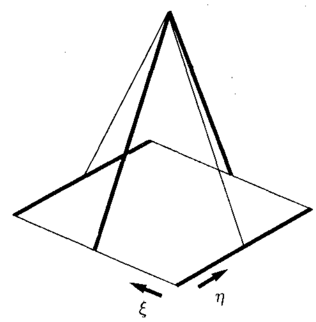

b) Topology of surface grid

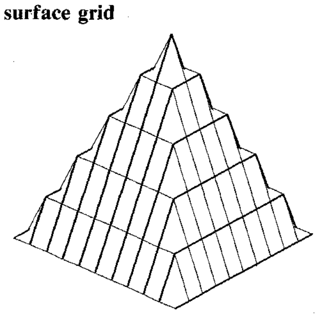

c) Surface grid

Fig. 2 Surface grid on a pyramid.

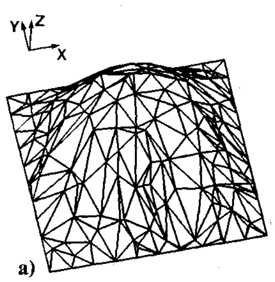

a)

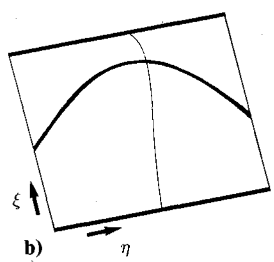

b)

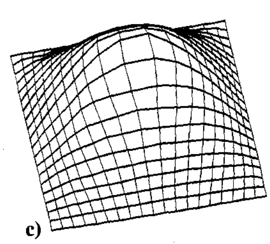

c)

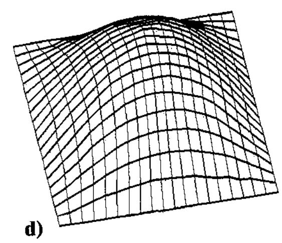

d)

Fig. 3 Effect of weight function λ on surface grid of $z = \sin x \sin y$: a) unstructured grid; b) topology of surface grid; c) surface grid, weight function λ = const; d) surface grid, weight function λ is proportional to the radius of curvature.

cult to describe the surface with discontinuities by a single patch using surface parametric coordinates. Simply dividing the surface into a number of local patches is ineffective, since there are grid cells extending over two side surfaces at the edges of the side surfaces of the pyramid. The present method, which can deal with plural patches, treats this problem easily. The effect of the weight function λ is seen in Fig. 3. The surface of $z = \sin x \sin y$ is examined. In Fig. 3c, $\lambda = \text{const}$; however, in Fig. 3d, λ is set to be proportional to the radius of the curvature. The clustering is performed successfully around the top of the curve without changing the point distribution on the boundary.

Summary

A new method of generating the surface grid has been presented. The capabilities of generating the smooth surface grids from the unstructured grid are demonstrated. An adaptive control of the mesh clustering is achieved by using the weight function. The accuracy of the surface definition is expected to improve further if the high-order patches are introduced.

Acknowledgments

The author deeply acknowledges S. Shirayama of the Institute of Computational Fluid Dynamics for his discussions. He is also grateful to J. M. Hyun of the Korea Advanced Institute of Science and Technology.

References

[1]Lee, K. D., and Loellbach, J. M., "Geometry-Adaptive Surface Grid Generation Using a Parametric Projection," AIAA Paper 88-0522, Jan. 1988.

[2]Luh, R. C. C., "Surface Grid Generation for Complex Three-Dimensional Geometries," *Numerical Grid Generation in Computational Fluid Dynamics '88,* Pineridge, Swansea, England, 1988, pp. 85–94.

[3]Rao, V. C. V., Sundararajan, T., and Das, P. C., "A New Approach to Grid Generation Using Finite Element Technique," *Numerical Grid Generation in Computational Fluid Dynamics '88,* Pineridge, Swansea, England, 1988, pp. 157–166.

[4]Thompson, J. F., Warsi, Z. U. A., and Mastin, C. W., *Numerical Grid Generation: Foundations and Applications,* Elsevier, New York, 1985, Chap. 6.

[5]Murata, K., Oguni, T., and Karaki, Y., *Supercomputer Applications to Scientific Computation,* Maruzen, Tokyo, 1985 (in Japanese), pp. 141–149.

Similarity Solutions for Supersonic Axisymmetric Flows

Hamdi T. Hemdan*
King Saud University, Riyadh 11451, Saudi Arabia

Introduction

IT is well known that similarity solutions exist in several areas of gasdynamics, including unsteady one-dimensional and steady hypersonic flow past slender axisymmetric and two-dimensional bodies. For such bodies, Sedov[1] has shown that the solutions have power-law shock waves and negligible freestream pressure. His work was later reviewed by Mirels[2] with emphasis on hypersonic flow. Cole and Aroesty[3] have shown that, for two-dimensional flow, the hypersonic small disturbance theory (HSDT) permits another similarity solution with exponential shock waves.

Received Jan. 8, 1990; revision received Oct. 17, 1990; accepted for publication Oct. 23, 1990.

*Associate Professor, Mathematics Department.

Later, Hui[4] found another similarity solution with logarithmic shock waves for two-dimensional flow. Both solutions,[3,4] similar to that of Sedov, assumed infinite M_∞. To show the effect of finite values of M_∞, Hui and Hemdan[5] perturbed the two solutions[3,4] and reduced the perturbation equations to ordinary differential equations. Here, we give new similarity solutions based on a recently developed hypersonic theory given in Ref. 6.

Perturbation Theory

The problem of hypersonic flow past pointed-nose slender axisymmetric bodies at zero incidence was approximated[6] as follows:

$$\hat{p}_x + (\hat{p}v)_r + \hat{p}v/r = 0 \tag{1a}$$

$$n\hat{p}_r + \hat{p}(v_x + vv_r) = 0 \tag{1b}$$

$$v[x,F(x)] = F'(x) \tag{2}$$

$$\hat{p}[x,S(x)] = S'^2(x) \tag{3a}$$

$$v[x,S(x)] = S'(x) - n/S'(x) \tag{3b}$$

where

$$n = 1/[1 + (\gamma - 1)M_\infty^2/2]$$

γ is the ratio of the specific heats of the gas, and $\hat{p}$, v, F, and S are, respectively, nondimensional: pressure, transverse speed, body, and shock wave. The variables $\hat{p}$, v, and S are related to the physical values $\bar{p}$, $\bar{v}$, and $\bar{S}$ by the following perturbation expansion:

$$\bar{p}(\bar{x},\bar{r}) - P_\infty = \rho_\infty U_\infty^2[\epsilon\hat{p}(x,r) - \epsilon n) + O(\epsilon^2)] \tag{4b}$$

$$\bar{v}(\bar{x},\bar{r}) = U_\infty[\sqrt{\epsilon}v(x,r) + O(\epsilon^{3/2})] \tag{4b}$$

$$\bar{S}(\bar{x}) = l[\sqrt{\epsilon}S(x) + O(\epsilon^{3/2})] \tag{4c}$$

where x and r are the physical axial and radial coordinates (see Fig. 1); P_∞, ρ_∞, and U_∞ the freestream pressure, density, and speed; l the body length; and ϵ the perturbation parameter defined by

$$\epsilon = \frac{\gamma - 1}{\gamma + 1} + \frac{2}{(\gamma + 1)M_\infty^2} \tag{5}$$

Finally, x and r are nondimensional coordinates defined by

$$x = \bar{x}/l \tag{6a}$$

$$r = \bar{r}/l\sqrt{\epsilon} \tag{6b}$$

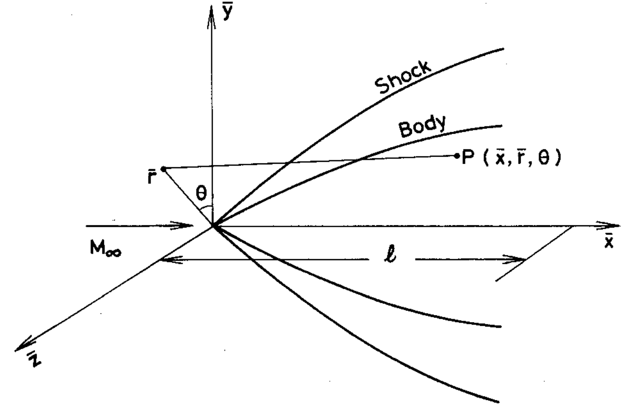

Fig. 1 Axisymmetric body and coordinates.